ISSN 2070-2051, Protection of Metals and Physical Chemistry of Surfaces, 2017, Vol. 53, No. 2, pp. 241–247. © Pleiades Publishing, Ltd., 2017.
Original Russian Text © A.S. Vishnevskii, A.E. Chalykh, S.A. Pisarev, V.K. Gerasimov, 2017, published in Fizikokhimiya Poverkhnosti i Zashchita Materialov, 2017, Vol. 53, No. 2, pp. 153–159.

NANOSCALE AND NANOSTRUCTURED MATERIALS AND COATINGS

The Structure of Individual Macromolecules of Butadiene–Styrene Copolymers in Polystyrene Matrix

A. S. Vishnevskii, A. E. Chalykh, S. A. Pisarev, and V. K. Gerasimov

Frumkin Institute of Physical Chemistry and Electrochemistry, Russian Academy of Sciences, Moscow, 119071 Russia

e-mail: trust-no-one@mail.ru

Received July 1, 2016

Abstract—Radial-density distribution functions of segments and radii of gyration are obtained for the first time with the example of systems of statistical butadiene–styrene rubber of different composition and polystyrene by the processing of electron-microscopy images of individual copolymer molecules. Linear correlation dependences of $R = f(M^{1/2})$ are plotted. The possibility of quantitative determination of fluctuation deviation from the equilibrium radius value is demonstrated. A method of calculating the values of Flory–Huggins parameters for individual macromolecules and their assembly is suggested.

DOI: 10.1134/S2070205117020265

INTRODUCTION

At present, there are a variety of physicochemical methods that allow studying the structural characteristics of macromolecules and determining their structure and particular details of their conformational arrangement [1]. Such methods include X-ray structural analysis [2], small–angle neutron scattering [3–5], small-angle X-ray scattering [6], nuclear magnetic resonance [7], and atomic-force microscopy [8].

Modern analytical transmission electron microscopy (TEM) is also one of the most informative methods of studying structural characteristics of materials [9–13]. It is commonly known that the TEM technique is based on analysis of the results of electron-beam scattering when it passes a given object, including individual macromolecules of biological or synthetic origin. Let us indicate that the modern technical support of image registration is characterized by new (digital) options for its processing and analysis.

The aim of this work was to obtain information on the structural characteristics of amorphous statistical copolymers of butadiene and styrene (SKS) dissolved in a polystyrene (PS) matrix by analysis of electron-microscopy images of individual copolymer macromolecules.

EXPERIMENTAL

The research objects were SKS-45[1] (M_w = 100 kDa), SKS-96 (M_w = 100 kDa), and PS (M_w = 230 kDa).

[1] The number used with SKS corresponds to percentage of styrene links.

The initial polymer solutions were prepared by dissolution in toluene at room temperature for 3–4 days under periodic stirring. The solutions were then mixed together at a ratio that provided a mixture of polymers with a given composition after removing the solvent (0.1, 0.05, 0.025, 0.01 wt % of SKS in PS).

Films of polymer mixtures SKS-45-PS and SKS-96-PS were obtained by pouring onto the surface of water under normal conditions. After the solvent was removed, PS films with a thickness of approximately 60–100 nm with distributed copolymer macromolecules were obtained. The films were annealed for several hours near the glass-transition point of PS for the maximum possible approximation to the equilibrium state of copolymer macromolecules and PS.

It was shown in our previous papers [14, 15] that the concentrations of 0.025 and 0.01 wt % are much lower than C^* (coil overlapping concentrations according to de Gennes [16]); i.e., the obtained films correspond to extremely diluted solutions of butadiene–styrene copolymers in PS, where interaction between copolymer macromolecules is practically absent.

Figure 1 shows a diagram of the amorphous layering of the SKS-45–PS system, coil overlapping concentration C^*, and imaging point C of the studied system. The inset shows the studied region in detail. The SKS-96–PS system is fully compatible in the temperature range of preparation and research.

Various contrasting techniques are used to obtain TEM images of biological and synthetic objects. To this purpose, negative contrasting with salts of phosphotungstic acid, molybdenum acetate, and uranyl acetate is used [18]. The fast and simple method of

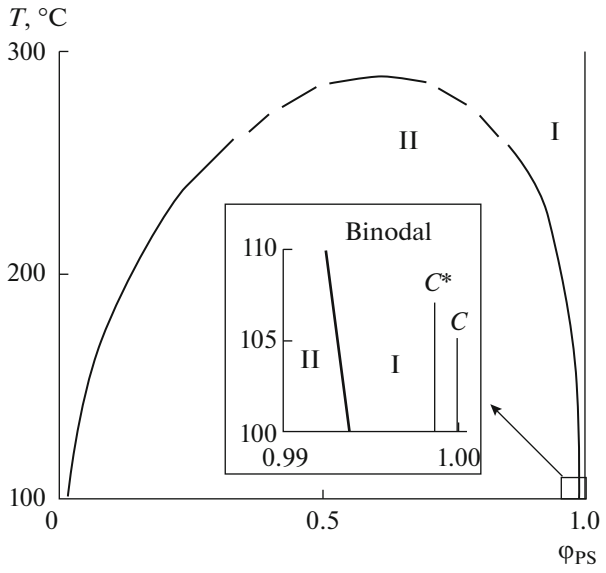

Fig. 1. Amorphous layering diagram of the SKS-45–PS system [17]. The inset shows bimodal C^*; C is the copolymer concentration used in the study. I, II are the single–phase and biphase regions, respectively.

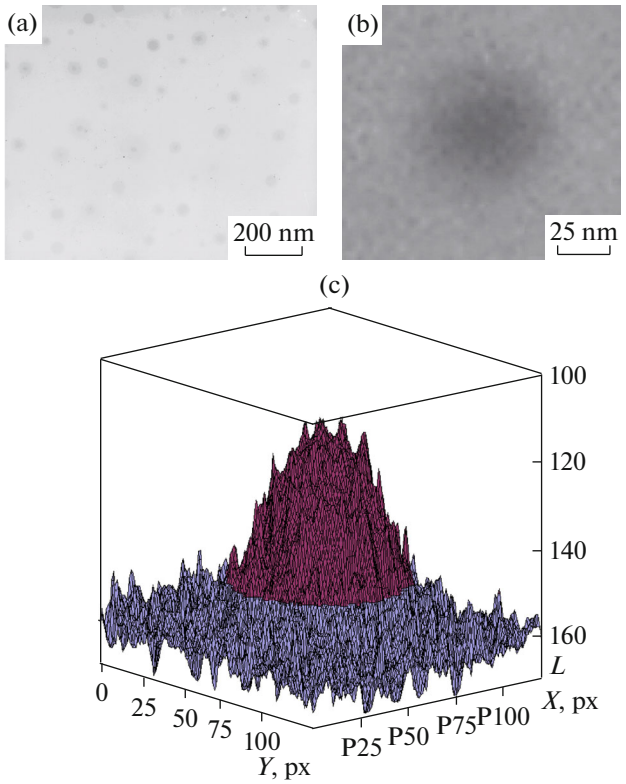

Fig. 2. Electron microphotograph of (a) SKS-45 macromolecules in a polystyrene matrix, (b) an individual macromolecule, and (c) the corresponding distribution of gray levels over the macromolecule image area. The concentration is 0.01 wt %.

negative contrasting provides fast enhancement of the contrast of the object, but causes distortion of macromolecules after drying. In this connection, we used contrasting of the object (copolymer) in an already-vitrified matrix, thus registering the conformation state of the copolymer.

Films were contrasted in OsO_4 vapors according to the standard technique from [19]. It is known that osmium tetraoxide reacts selectively with double bonds of butadiene links of copolymers [20]. Electron-microscopy studies were carried out using an EM-301 transmission electron microscope (Philips). Measurements were performed using the bright-field method at an accelerating voltage of 60–100 KeV. The resolution was 0.5 nm.

From 150 to 250 images of individual macromolecules were obtained and processed in the course of electron-microscopy studies for every copolymer.

The inelastic light-scattering technique was used to obtain independent information on the molecular-mass distribution of copolymers. Measurements were carried out[2] using a Malvern Zetasizer Nano device for infinitely diluted copolymer solutions in toluene.

RESULTS AND DISCUSSION

Figure 2 contains a typical microphotograph of the copolymer of SKS-45 in a polystyrene matrix as an example. Microphotographs show pronounced objects, which are presumably individual copolymer macromolecules. However, this hypothesis has to be confirmed.

First, it is conventionally assumed in physical chemistry of polymers that the size and molecular-mass distributions of macromolecules are constant at concentrations below C^*. Indeed, when the SKS concentration in PS decreases from 0.1 to 0.025 wt %, particle-size-distribution histograms change and shift toward lower values, while for concentrations of 0.025 and 0.01 wt % all histograms are rather close, i.e., dilution in this concentration range results in no change in the particle-size and molecular-mass distributions, which fulfils the above requirement.

Second, since osmium tetraoxide reacts quantitatively with the double bonds of butadiene links in SKS, all cases of exceeding the background level of the image-blackening degree (Fig. 2c) indicate that the nanoobject is a copolymer containing double bonds. It is shown in previous works [15] that the blackening degree of the image of an individual macromolecule is directly related to the content of double bonds in statistical butadiene–styrene copolymers.

Obviously, the overall excess of the blackening degrees over the background values for an individual copolymer dissolved in a PS matrix (blackening inte-

[2] We are grateful to Dr. Sci. (Physics and Mathematics) V.D. Sobolev for providing the possibility of performing the measurements.

gral F) is directly related to the molecular mass of the specific polymer molecule. The blackening integrals of the whole processed set of images of individual macromolecules registered under similar conditions of electron-microscopy measurements are proportional to the molecular mass distribution of the studied copolymers.

Figure 3 shows histograms of radius distribution for macromolecules dissolved in toluene and $F^{1/2}$ of all the processed images of macromolecules (the macromolecule coil radius is proportional to the square root of MM and, thus, also of F). One can see that both characteristics agree with each other.

Thus, one can state that the nanoobjects observed in the microphotographs are, indeed, individual macromolecules. Earlier, a similar technique was used for studying macromolecules of polybutadiene in the PS matrix [14].

As already pointed out above, integrals of blackening are proportional to the molar mass distribution. This means the possibility of calculating the number-average (F_n) and mass-average (F_w) characteristics of distribution of F. The results of calculation are shown in Fig. 4. The same figures show the curves of normal logarithmic distribution describing histograms of distribution of the blackening integrals.

The independent value of M_w and of F_w calculated using the distribution allows determining the molecular mass of each macromolecule. This information is necessary for calculation of the radial density distribution function of segments and the radius of gyration of the polymer coil. To this end, blackening function f is determined by summation over one of the coordinates of gray levels. As shown in Fig. 5a, this function is symmetrical with respect to the mass center for centrally symmetric objects, which allows averaging the right and left parts of the curve (Fig. 5b).

The further calculation of the radial-density distribution function was carried out according to the following equation [21]:

$$\rho(r) = -\frac{\frac{\partial f}{\partial r}}{2\pi r}. \qquad (1)$$

Here, $\rho(r)$ is the radial-density distribution function and r is the current radius.

Figure 6 shows a typical radial-density distribution function of segments of the SKS-45 macromolecule. Analysis of radial distribution functions, their average values, and fluctuation deviations from the average requires a separate study. It is important for us that the knowledge of the radial-density distribution function allows calculation of the radius of gyration using the standard numeric methods. Such a calculation was carried out for all the studied images of polymer macromolecules.

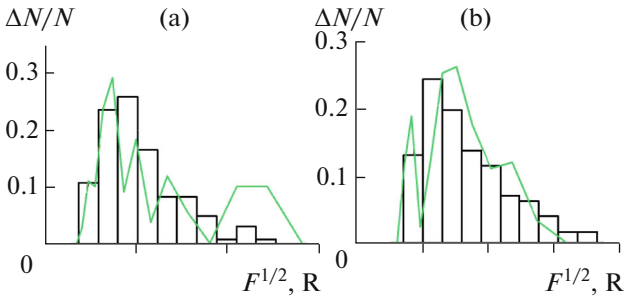

Fig. 3. Distribution of radii according to the data of inelastic light scattering (green). Histogram of distribution of blackening functions $F^{1/2}$ (black) for (a) SKS-96 and (b) SKS-45.

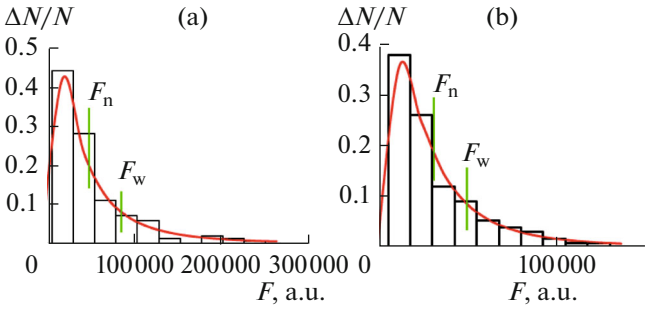

Fig. 4. Molecular mass distribution of styrene copolymers of (a) SKS-96 and (b) SKS-45.

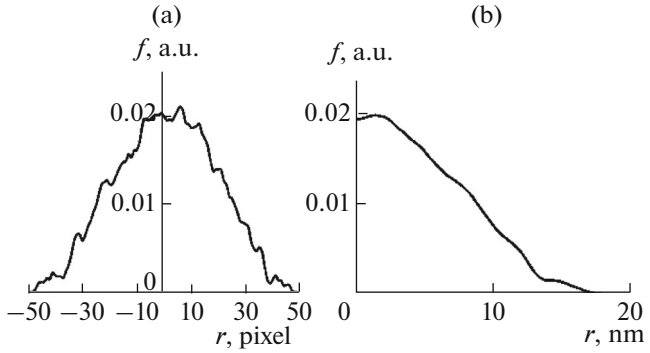

Fig. 5. (a) Blackening function obtained from the digital image of the macromolecule (b) averaged with respect to the mass center.

The obtained results are of fundamental importance for estimation of the equilibrium and fluctuating state of specific macromolecules. To this end, we suggest using the correlation dependence of the radius of gyration on the square root of MM (Fig. 7).

It appeared necessary to supplement the experimentally found dependences by information on radii of gyration of macromolecules on their $MM^{1/2}$ in the θ-state. We used reference data for their calculation

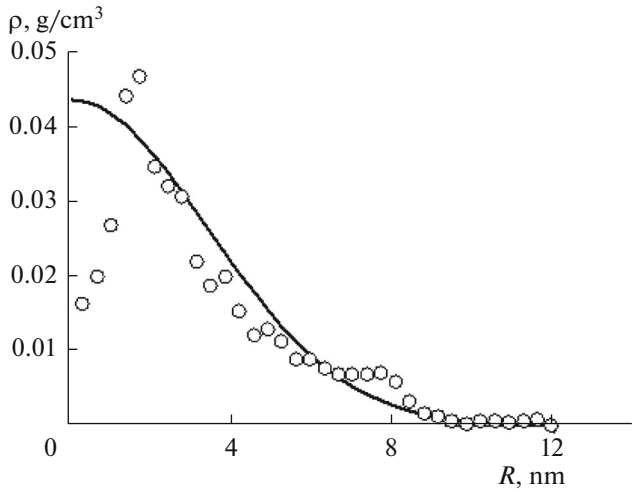

Fig. 6. Radial-density distribution function of macromolecule segments (dots) and its description according to the equation (line).

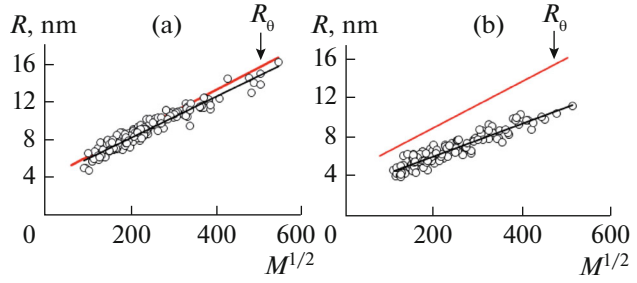

Fig. 7. Experimental dependence of the radius of gyration on the blackening for the (a) SKS-96 and (b) SKS-45 macromolecules. The red line shows extrapolation corresponding to the unperturbed state of the coil.

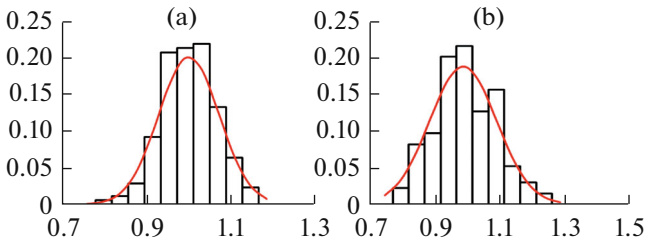

Fig. 8. Histograms of distribution for the ratios of radii of gyration of specific macromolecules to the equilibrium radii of gyration and normal distribution curves. (a) SKS-96 and (b) SKS-45.

[22, 23]. In the cases in which the data on the θ-state were absent, the dependence was calculated on the basis of the dependences of $R = f\left(M^{1/2}\right)$ for specific solvents and correction for the swelling degree of macromolecular coils was introduced.

As seen from Fig. 7, all experimental points form a rather narrow range of values. For the studied macromolecules, the radii of gyration varied from 3 to 14 nm with an average of 7 nm for SKS-45 and from 3 to 16 nm with the average of 9 nm for SKS-96. A decrease in the average radius of the SKS-45 macromolecules as compared to SKS-96 is related to the different distance of the image points of the studied systems from their binodal curves, which can also be related to a decrease in solubility in polystyrene of butadiene–styrene rubbers at an increase in the content of butadiene groups [24, 25].

The deviation of the radius of a specific macromolecule from its equilibrium radius is a manifestation of the density fluctuation. Figure 8 shows the histograms of distribution for the ratios of the radius of gyration of a specific macromolecule to the equilibrium radius of a copolymer macromolecule with the same molecular mass. The same figure contains the normal distribution curves. One can see that the histograms are rather well described by the normal distribution. The normal-distribution dispersions (σ^2) for SKS-96 and SKS-45 are 0.0051 and 0.0104, respectively. Differences in dispersions are probably related to the fact that compatibility of SKS-45 with PS is much worse than that of SKS-96 with PS [24], as already pointed out above.

Information on equilibrium radii of gyration and radii of gyration in the θ-state allows calculating thermodynamic characteristics of interaction between copolymers and PS.

The expression relating the thermodynamic characteristics of interaction and variation of the polymer coil size with respect to the θ-state is known from the literature [1, 26, 27]:

$$2C_{\mathrm{m}}\psi\left(1-\theta/T\right)M^{1/2} \approx 4/3\,z. \qquad (2)$$

Here, $\psi(1-\theta/T) = -\chi$ is the Flory–Huggins interaction parameter, z is a dimensionless parameter related to swelling degree $\alpha = R/R_\theta$, and C_{m} is the parameter related to molecular characteristics of the swelling or contracting macromolecule. Parameter C_{m} is

$$C_{\mathrm{m}} = K\left(\vec{V}^2/N_A V_0\right)\left(\langle h^2\rangle_0/M\right)^{-3/2}, \qquad (3)$$

where $K = 27/2^{5/2}\pi^{3/2}$, $\vec{V}$ is the partial molar volume, V_0 is the molar volume of the polymer, $\langle h^2\rangle_0$ is the mean square of the radius of gyration in the θ-state, and M is the molecular mass of the polymer.

Several empirical equations relating parameter z and swelling degree α are known [1]. In our previous work [28], we compared the results of the numeric modeling of conformations of an individual macromolecule with the known equations relating parameters z and α and concluded that the best equation for making predictions is the Kurata–Aleksandrovich equation [1]:

$$\alpha^3 - 1 + 3/8(\alpha^5 - \alpha^3) = 5/2\,z \quad (4)$$

However, the above is insufficient for calculation of the Flory–Hyggins parameter. Parameter C_m includes partial molar volume $\vec{V}$ of the copolymer. Determining it for the studied copolymers appears to be impossible.

The dependence describing the radial density distribution of segments is known from the literature [29]:

$$\rho(r) = n\left[\frac{3}{2\pi R^2}\right]^{\frac{3}{2}} \exp\left[-\frac{3r^2}{2R^2}\right], \quad (5)$$

where $\rho(r)$ is the radial segment distribution density, n is the number of monomer links in a macromolecule, R is the radius of gyration of a macromolecule, r is the current radius. Accordingly, the radial-segment density function takes the following form in the mass center:

$$\rho(0) = n\left[\frac{3}{2\pi R^2}\right]^{\frac{3}{2}}. \quad (6)$$

Earlier, we used the data of numeric modeling to obtain an empirical equation relating the Flory–Huggins parameter and segment density in the mass center of the polymer coil [28]. This expression takes the following form:

$$(\rho_{0,\varepsilon} - \rho_{0,0}) = 16\chi^2 + 2\chi, \quad (7)$$

where $\rho_{0,\varepsilon}$ and $\rho_{0,0}$ are the radial segment density functions in the mass center of the θ-coil and of the coil interacting with the matrix, respectively. The range of application of this equation is small, but allows calculating the partial molar volume of the copolymer and necessary parameter C_m using the earlier-determined radii of gyration of macromolecules and their molecular masses.

After the preliminary calculations of parameter C_m, Eqs. (2)–(4) were used to determine the values of Flory–Huggins parameters for individual macromolecules, images of which were processed and to obtain the average values and the average distribution. Figure 9 shows histograms of distribution of the Flory–Huggins parameter and description of the histograms by the normal-distribution equation. One can see that the Flory–Huggins parameter is close to zero for SKS-96; i.e., on average, there is practically no interaction. At the same time, the fluctuating coils deviate rather strongly from the equilibrium state both toward swelling ($\chi < 0$) and towards contraction ($\chi > 0$). For SKS-45, the value of the Flory–Huggins parameter is much higher (0.02) (Fig. 9b). This corresponds to deterioration of compatibility of butadiene–styrene copolymers with PS at an increase in the content of butadiene links. The cause of the worse agreement of the distribution with the normal distribution function is unclear and requires additional study. As could be expected, dispersion of the distribution for SKS-96 is much lower than for SKS-45 (6.8×10^{-6} and 6.3×10^{-5}, respectively). Density fluctuations and the related interaction fluctuations probably depend on the average interaction value. One must also indicate that, in our opinion, the obtained thermodynamic characteristics must be attributed to the glass-transition point of PS (100–105°C). It is at this temperature that the structure of the statistic copolymer is fixed by vitrification of the matrix.

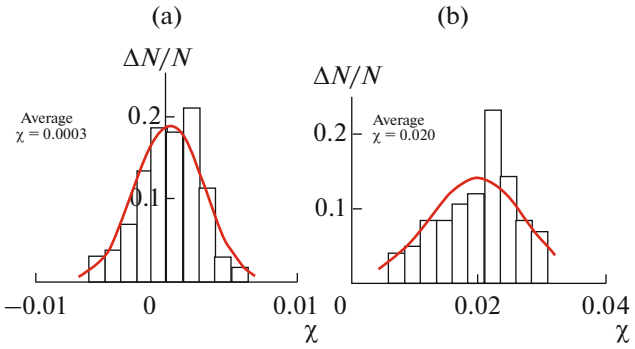

Fig. 9. Histograms of distribution of pair interaction parameter for macromolecules of (a) SKS-96 and (b) SKS-45. The continuous line corresponds to the normal distribution.

Studies of interaction between the polymer components without involving any third components (common solvents) is a rather complicated experimental problem. There are few experimental techniques providing direct thermodynamic information on interaction of polymer pairs. This set includes analysis of phase-state diagrams. Earlier [17], we suggested carrying out thermodynamic analysis of binodal curves based on the theory of polymer solutions of Flory–Huggins [30, 31], which was extended by Scott to the polymer mixture [32]. According to the suggested analysis, the compositions of the coexisting phases and polymerization degree of components are related to the pair-interaction parameter (Flory–Huggins parameter) by the following relationship:

$$\chi = \frac{\dfrac{\ln\left(\dfrac{\varphi_1''}{\varphi_1'}\right)}{r_1} - \dfrac{\ln\left(\dfrac{\varphi_2''}{\varphi_2'}\right)}{r_2}}{2\left(\varphi_2'' - \varphi_2'\right)}. \quad (8)$$

Here, χ is the pair-interaction parameter; φ_i is the bulk concentration of component i; subscripts ' and " correspond to the first and second phases, respectively; and r_i is the polymerization degree of component i. The compositions of the coexisting phases correspond to the isothermal section of the amorphous layering diagram. Calculation of the Flory–Huggins

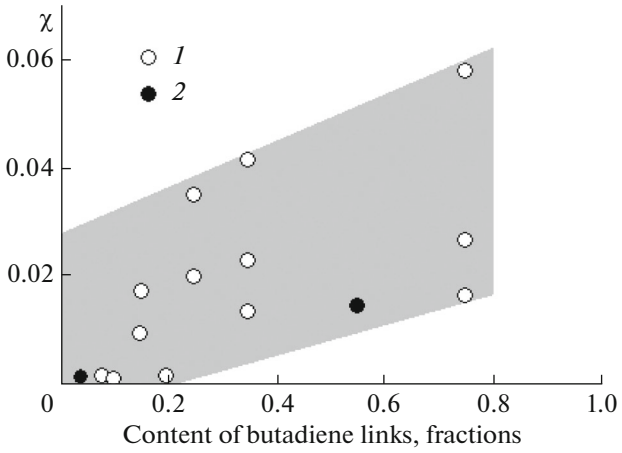

Fig. 10. Dependence of the pair interaction parameter in the system of PS–SKS on the composition of butadiene–styrene copolymers. (*1*) Analysis of amorphous layering, (*2*) this work.

parameters according to Eq. (8) for different temperatures allows plotting the temperature dependence of χ.

Paper [33] contains the above-described thermodynamic analysis of binodal curves of the systems of PS–polybutadiene (PB), PS–SKS, and SKS–SKS of different molecular masses. Figure 10 shows the results of such analysis. The same figure presents the values of Flory–Huggins parameters obtained in this work. It is shown that the above results with all the above assumptions do not contradict the data obtained using a different method.

CONCLUSIONS

Thus, radial-density distribution functions of segments and radii of gyration are obtained by the processing of electron-microscopy images of individual macromolecules of statistical butadiene–styrene copolymers distributed in a PS matrix. Linear correlation dependences of $R = f(M^{1/2})$ are plotted. The possibility of quantitative determination of fluctuation deviation from the equilibrium radius value is demonstrated. A method of calculating the values of Flory–Huggins parameters for individual macromolecules and their assembly is suggested.

ACKNOWLEDGMENTS

This work was financially supported by the Russian Foundation for Basic Research, project no. 14-03-00390.

REFERENCES

1. Dashevskii, V.G., *Konformatsionnyi analiz makromolekul* (Conformational Analysis for Macromolecules), Moscow: Nauka, 1987.
2. Goryacheva, E., *Biologiya,* 2009, no. 4, p. 2; no. 5, p. 26.
3. Svergun, D.I. and Feigin, L.A., *Rentgenovskoe i neitronnoe malouglovoe rasseyanie* (Low-Angle X-Ray and Neutron Scattering), Moscow: Nauka, 1986.
4. Ostanevich, Yu.M. and Serdyuk, I.N., *Usp. Fiz. Nauk,* 1982, vol. 137, p. 85.
5. Lebedev, V.T., et al., *Polym. Sci., Ser. A,* 2009, vol. 51, p. 372.
6. Svergun, D.I., et al., *Crystallogr. Rep.,* 2011, vol. 56, p. 725.
7. *Derome, A.E., Modern NMR Techniques for Chemistry Research,* New York: Pergamon, 1987.
8. Gallyamov, M.O., *Doctoral Sci. (Phys.-Math.) Dissertation,* Moscow: Moscow State Univ., 2009.
9. Sokolova, O.S., Volokh, O.I., Stanishneva-Konovalova, T.B., and Pechnikova, E.V., *Integral,* 2012, vol. 5, p. 22.
10. Koval'chuk, M. and Popov, V., Nauka Ross., 2013, no. 3, p. 4.
11. Staniewicz, L., Donald, A.M., and Stokes, D.J., *J. Phys.: Conf. Ser.,* 2010, vol. 241, p. 012077.
12. Shindo, D. and Oikawa, T., *Analytical Electron Microscopy for Materials Science*, Tokyo: Springer, 2002.
13. Pechnikova, E.V., Stanishneva-Konovalova, T.B., Volokh, O.I., and Sokolova, O.S., *Nanoindustriya,* 2013, vol. 43, p. 18.
14. Busygin, V.B., *Cand. Sci. (Chem.) Dissertation,* Moscow: Inst. of Physical Chemistry USSR Acad. Sci., 1989.
15. Alekseenko, T.V., *Cand. Sci. (Chem.) Dissertation,* Moscow: Inst. of Physical Chemistry Russ. Acad. Sci., 1995.
16. *de* Gennes, P.-G., *Scaling Concepts in Polymer Physics*, Ithaca, NY: Cornell Univ. Press, 1979.
17. Chalykh, A.E., Gerasimov, V.K., and Mikhailov, Yu.M., *Diagrammy fazovogo sostoyaniya polimernykh sistem* (Phase State Diagrams for Polymer Systems), Moscow: Yanus-K, 1998.
18. Harris, J.R., *Micron,* 2002, vol. 33, p. 609.

19. Schimmel, G., *Methodensammlung der Elektronenmikroskopie,* Stuttgart: Wissenschaftliche Verlagsgesellschaft, 1970.
20. Dogadkin, B.A., Dontsov, A.A., and Shershnev, V.A., *Khimiya elastomerov* (Chemistry of Elastomers), Moscow: Khimiya, 1981.
21. Gerasimov, V.K. and Chalykh, A.E., *Polym. Sci., Ser. B,* 2001, vol. 43, p. 307.
22. *Polymer Data Handbook,* Mark, J.E., Ed., New York, NY: Oxford Univ. Press., 1999.
23. Nesterov, A.E., *Spravochnik po fizicheskoi khimii polimerov* (Physical Chemistry of Polymers. Handbook), Kiev: Naukova Dumka, 1984, vol. 1.
24. Chalykh, A.E., *Diagrammy fazovykh sostoyanii polimernykh sistem* (Phase State Diagrams for Polymer Systems), Moscow: Inst. of Physical Chemistry Russ. Acad. Sci., 1995.
25. Roe, R.-J. and Zin, W.Ch., *Macromolecules,* 1984, vol. 17, p. 189.
26. Grosberg, A.Yu. and Khokhlov, A.R., *Statisticheskaya fizika makromolekul* (Statistical Physics of Macromolecules), Moscow: Nauka, 1989.
27. Tager, A.A., *Fizikokhimiya polimerov* (Physical Chemistry of Polymers), Moscow: Khimiya, 1978.
28. Vishnevskii, A.S., Chalykh, A.E., and Gerasimov, V.K., *Vestn. Kazan. Tekhnol. Univ.,* 2013, no. 1, p. 246.
29. Semchikov, Yu.D., *Vysokomolekulyarnye soedineniya* (High-Molecular Compounds), Moscow: Akademiya, 2003.
30. Flory, P.J., *J. Chem. Phys.,* 1941, vol. 9, p. 660.
31. Huggins, M.L., *J. Chem. Phys.,* 1941, vol. 9, p. 440.
32. Scott, R.L., *J. Chem. Phys.,* 1949, vol. 17, p. 268.
33. Gerasimov, V.K., *Doctoral Sci. (Chem.) Dissertation,* Moscow: A.N. Frumkin Inst. of Physical Chemistry and Electrochemistry Russ. Acad. Sci., 2012.

Translated by M. Ehrenburg